Letter
Vol. 22, No. 6, p. 871–880, December 2018
https://doi.org/10.1007/s12303-018-0051-y
pISSN 1226-4806 eISSN 1598-7477
Geosciences Journal GJ

Paleoseismological implications of liquefaction-induced structures caused by the 2017 Pohang Earthquake

Yong Sik Gihm[1]*, Sung Won Kim[1], Kyoungtae Ko[2], Jin-Hyuck Choi[1], Hankyung Bae[1], Paul S. Hong[1], Yuyoung Lee[1], Hoil Lee[3], Kwangmin Jin[2], Sung-ja Choi[4], Jin Cheul Kim[3], Min Seok Choi[5], and Seung Ryeol Lee[1]

[1]Geology Division, Korea Institute of Geoscience and Mineral Resources, Daejeon 34132, Republic of Korea
[2]Climate Change Mitigation and Sustainability Division, Korea Institute of Geoscience and Mineral Resources, Daejeon 34132, Republic of Korea
[3]Geologic Environment Division, Korea Institute of Geoscience and Mineral Resources, Daejeon 34132, Republic of Korea
[4]Geoscience and Technology Dissemination Division, Korea Institute of Geoscience and Mineral Resources, 34132, Republic of Korea
[5]Department of Geological Science, Pusan National University, Busan 46241, Republic of Korea

ABSTRACT: During and shortly after the 2017 Pohang Earthquake (M_w 5.4), sand blows were observed around the epicenter for the first time since the beginning of instrumental seismic recording in South Korea. We carried out field surveys plus satellite and drone imagery analyses, resulting in observation of approximately 600 sand blows on Quaternary sediment cover in this area. Most were observed within 3 km of the epicenter, with the farthest being 15 km away. In order to investigate the ground's susceptibility to liquefaction, we conducted a trench study of a 30 m-long sand blow in a rice field 1 km from the earthquake epicenter. The physical characteristics of the liquified sediments (grain size, impermeable barriers, saturation, and low overburden pressure) closely matched the optimum ground conditions for liquefaction. Additionally, we found a series of soft sediment deformation structures (SSDSs) within the trench walls, such as load structures and water-escaped structures. The latter were vertically connected to sand blows on the surface, reflecting seismogenic liquefaction involving subsurface deformation during sand blow formation. This genetic linkage suggests that SSDS research would be useful for identifying prehistoric damage-inducing earthquakes (M_w > 5.0) in South Korea because SSDSs have a lower formation threshold and higher preservational potential than geomorphic markers formed by surface ruptures. Thus, future combined studies of Quaternary surface faults and SSDSs are required to provide reliable paleoseismological information in Korea.

Key words: sand blows, load structures, water-escaped structures, Quaternary, soft sediment deformation structures

Manuscript received April 16, 2018; Manuscript accepted September 3, 2018

1. INTRODUCTION

Liquefaction is the temporal transformation in the physical conditions of water-saturated granular sediments from a solid to viscous-fluid state as a result of increased pore water pressure (Obermeier, 2009). During moderate to strong earthquakes (M_w > 5.0), ground shaking causes the grain rearrangement with a rapid decrease in pore space. If an impermeable cap covers the liquefied sediments, the increased pore pressure supports the weight of grains, and sediments lose their own strength, resulting in a temporary change in physical conditions (Maltman and Bolton, 2003; Owen, 2003; Owen et al., 2011). When the pore water pressure exceeds the strength of the overlying impermeable cap, a mixture of water and sediments is vented to the surface, forming sand blows (Sims, 1975; Obermeier, 2009; Rodríguez-Pascua et al., 2015). Such sand blows have been used to detect prehistoric earthquakes and provide paleoseismological information such as recurrence intervals and minimum magnitude (Obermeier, 1996; Galli, 2000; Tuttle et al., 2002; Castilla and Audemard, 2007), particularly in areas where seismogenic faults do not penetrate the surface (Rajaedran et al., 2001).

On November 15th, 2017, a moderate earthquake (M_w 5.4, depth: 3–4 km) occurred in the northern part of Pohang city, triggered by the reverse movement of subsurface fault(s) with minor strike-slip movement (KIGAM, 2018). Associated ground shaking resulted in widespread damage to buildings, roads,

*Corresponding author:
Yong Sik Gihm
Geology Division, Korea Institute of Geoscience and Mineral Resources, 124 Gwahak-ro Yuseong-gu, Daejeon 34132, Republic of Korea
Tel: +82-42-868-3239, Fax: +82-42-868-3413, E-mail: naress@kigam.re.kr

bridges, and walls, estimated at approximately KRW 55.1 billion (approximately US $52 million). During the earthquake, ground motion and resultant liquefaction caused the formation of a number of sand blows on the surface near the epicenter. These seismogenic sand blows were the first to have been observed since the beginning of instrumental seismic signal recording in South Korea.

In this study, we present geological information on the liquefaction-induced structures produced by the 2017 Pohang Earthquake and evaluate the liquefaction vulnerability of underground conditions near the epicenter by comparing subsurface sediment conditions determined by a trench study with the optimum underground conditions for liquefaction (Obermeier, 2009; Owen and Moretti, 2011). We also describe the soft sediment deformation structures (SSDSs) found in the trench walls and discuss their importance for paleoseismological research in South Korea.

2. LIQUEFACTION-INDUCED STRUCTURES

The 2017 Pohang Earthquake occurred in the central part of the Pohang Basin (KIGAM, 2018). The Pohang Basin is a Miocene sedimentary Basin in SE Korea, which began to open at about 17 Ma as a result of movement of western border faults (NNE-trending normal faults and NW-trending transfer fault, Sohn and Son, 2004) under WNW-ESE extensional stress field (Son et al., 2015). The Pohang basin fills are composed of poorly-consolidated marine sediments sourced mostly from a series of fan-delta systems distributed along the western border faults (Hwang et al., 1995). In the Late Miocene, the sedimentation ceased, and then the basin was uplifted by tectonic inversion (Son et al., 2015). The Miocene marine sediments are now exposed or covered unconformably by Quaternary fluvial and coastal sediments (Fig. 1). The Quaternary sediments are locally cut by reverse faults, particularly along or near the western border faults of the Pohang Basin (Kyung and Chang, 2001; Kim and Jin, 2006).

The day after the earthquake, we began a postseismic field investigation around the epicenter, together with drone imagery acquisition in order to identify sand blows. At the same time, we analyzed changes in ground conditions (e.g., surface wetting and large-scale vented sediment) after the mainshock based on

Fig. 1. Spatial distribution of the sand blows around the epicenter with the numbers of the sand blows away from the epicenter (top left). All sand blows occur only on the Quaternary sediments.

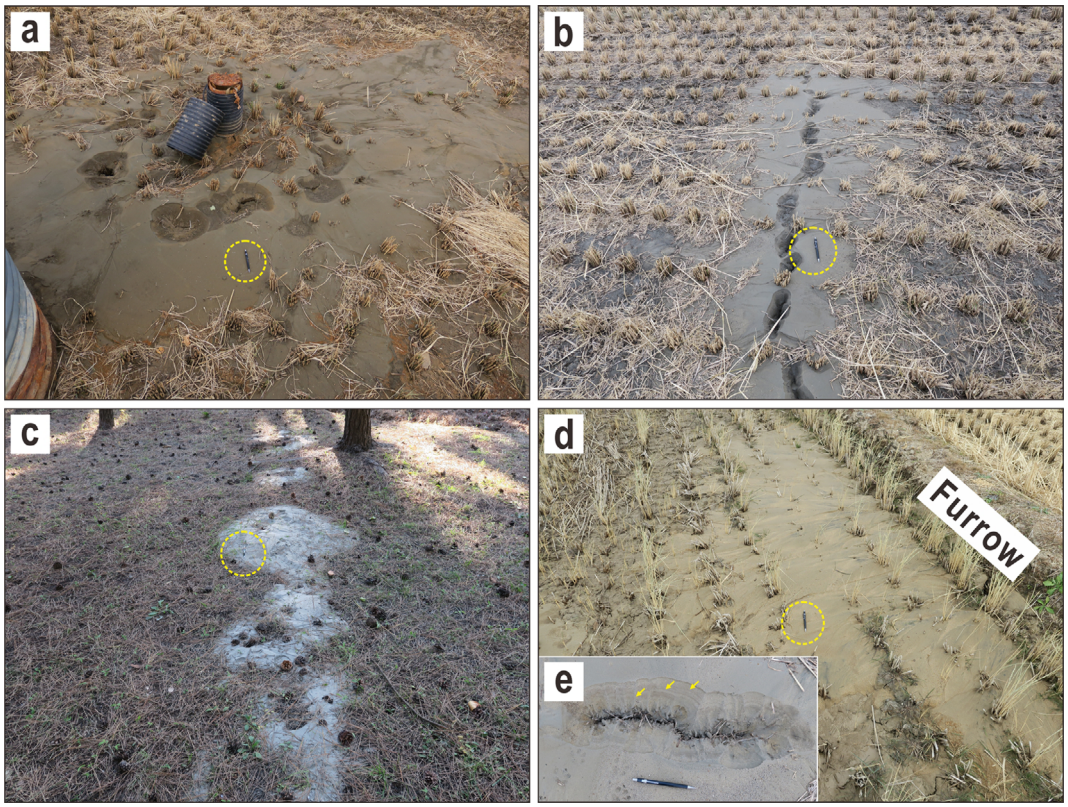

Fig. 2. Field photographs of sand blows. The observed sand blows can be classified into three types: subcircular, linear, and linear along the artifact. (a) Subcircular type contains one or multiple source vents in its central part. (b and c) Linear type is aligned parallel to surface cracks (b) or composed of linear arrangements of a series of subcircular types (c). (d) Linear along artifact type is bounded by artificial structures, such as waterway and furrows. (e) Internal structure of the sand blows. Some sand blows are composed of alternating thin layers of fine (mud to very fine sand) and coarse (fine to coarse sand) grains.

a comparison between preseismic and postseismic satellite imageries. Using these combined methods, we observed approximately 600 sand blows on Quaternary sediment cover (Fig. 1). Most were observed on rice fields within 3 km of the epicenter, with the farthest occurring 15 km away.

The sand blows have diverse shapes, which we classified into three types: subcircular, linear, and linear along an artifact (formed along human structures) (Fig. 2). The subcircular type has similar ratios between its long (L) and short (S) axes (mean L/S = 2.06) and ranges in diameter from 0.3 to 22 m (Fig. 2a). One or more source vents occur in the central part of this type. The linear type is generally elliptical (mean L/S = 4.9) (Figs. 2b and c). This type is composed of vented sediments sourced from surface cracks or linear alignments of multiple subcircular types, ranging in length (long axis) from 0.2–70 m (average 5.44 m) (Figs. 2b and c). This type comprises the majority of observed sand blows (Fig. 3a) and is preferentially oriented NNE-SSW (Fig. 4a), although they were more randomly distributed within 1 km of the epicenter (Fig. 4b). The last type has similar morphology to the linear type, but the sediments were extruded from cracks along man-made structures such as furrows, roads, and waterways (Fig. 2d).

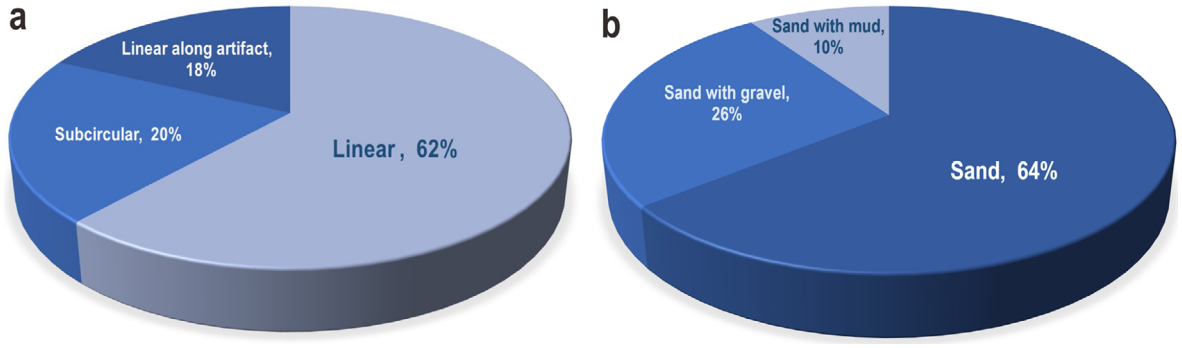

Fig. 3. The proportion of the sand blow types (a) and their constituent sediments (b).

https://doi.org/10.1007/s12303-018-0051-y

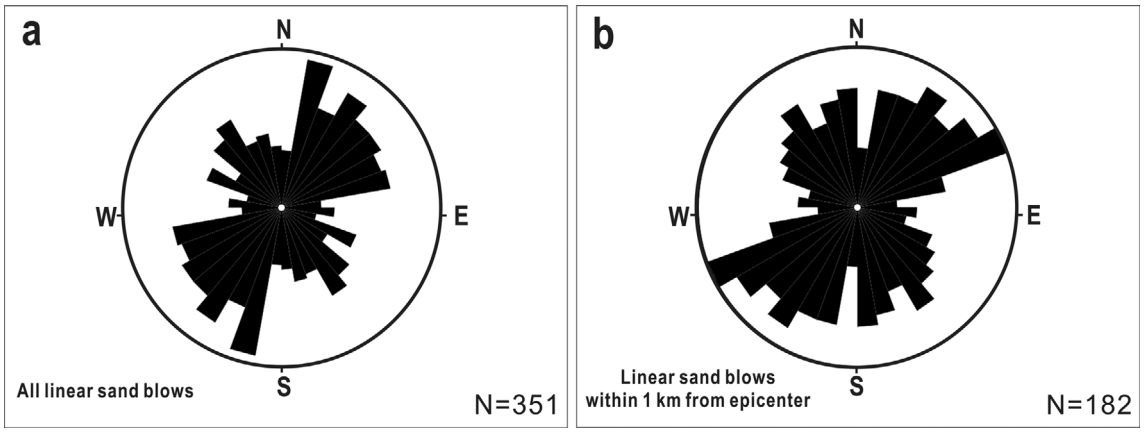

Fig. 4. Orientation of linear sand blows. The linear type is preferentially oriented in a NNE-SSW direction (a), although those within 1 km from the epicenter are somewhat randomly distributed (b).

The sand blows are composed of moderately to well-sorted sand, ranging in size from very fine to coarse (Fig. 3b). In some cases, the sand is covered by mud (silt and clay). Pebbles (rarely cobbles) are also scattered throughout the sand blows. Although most are structureless when viewed vertically, some are composed of two or three units of normally graded sand, with each divided by a few cm of silt or very fine sand (Fig. 2e). Although sand blows are commonly reported to involve ground disturbances, we found no evidence of subsidence or uplift in most rice fields. However, in Songdo-dong, the ground had subsided or risen by as much as 15 cm from the surface around the sand blows (Figs. 1 and 5).

3. TRENCH SURVEY

We conducted a trench survey to better understand ground conditions near the epicenter. The trench site is located 1 km from the epicenter, where a NE-SW trending linear sand blow is well-developed along a 30-m long axis (Fig. 6a). Although we planned to excavate to below 5 m depth from the surface, we were forced to stop at 2.5 m due to high discharge of groundwater from the sand beds (1.5–1.6 m below the surface) and resultant ground instabilities (Fig. 6b).

3.1. Stratigraphy

The underground sediments within the trench are loose and frangible enough to be scraped by a finger. Based on grain size and stacking patterns, these sediments were divided into two units (Fig. 7a) with a highly irregular boundary. Unit A, the uppermost part, is composed of entirely structureless silt and clay with scattered organic matters and pebbles. This unit is 1–1.6 m thick from the surface with no any break in grain size and shows only a gradual downward change in color from brownish grey to bluish grey.

Unit B is composed of alternating layers of sand and mud (Fig. 6c). The sand layers are a few cm to 25 cm thick and consist of moderately to well-sorted very fine to coarse sand (mainly

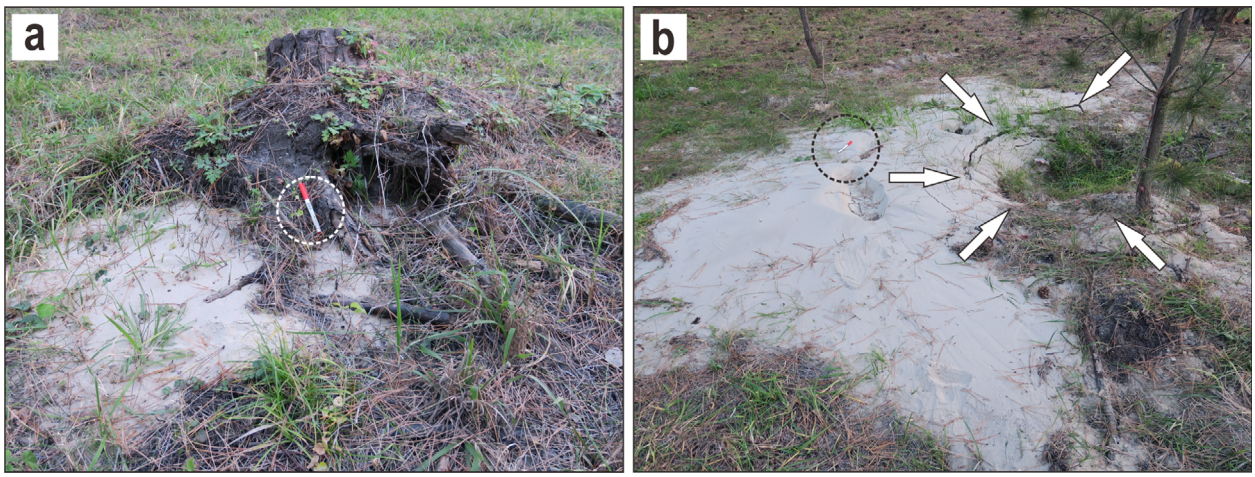

Fig. 5. Ground disturbances in Songdo-dong (Location indicated in Fig. 1). In this area, the sand blows involve ground disturbances: rise (a) and subsidence (b) indicated by arrows.

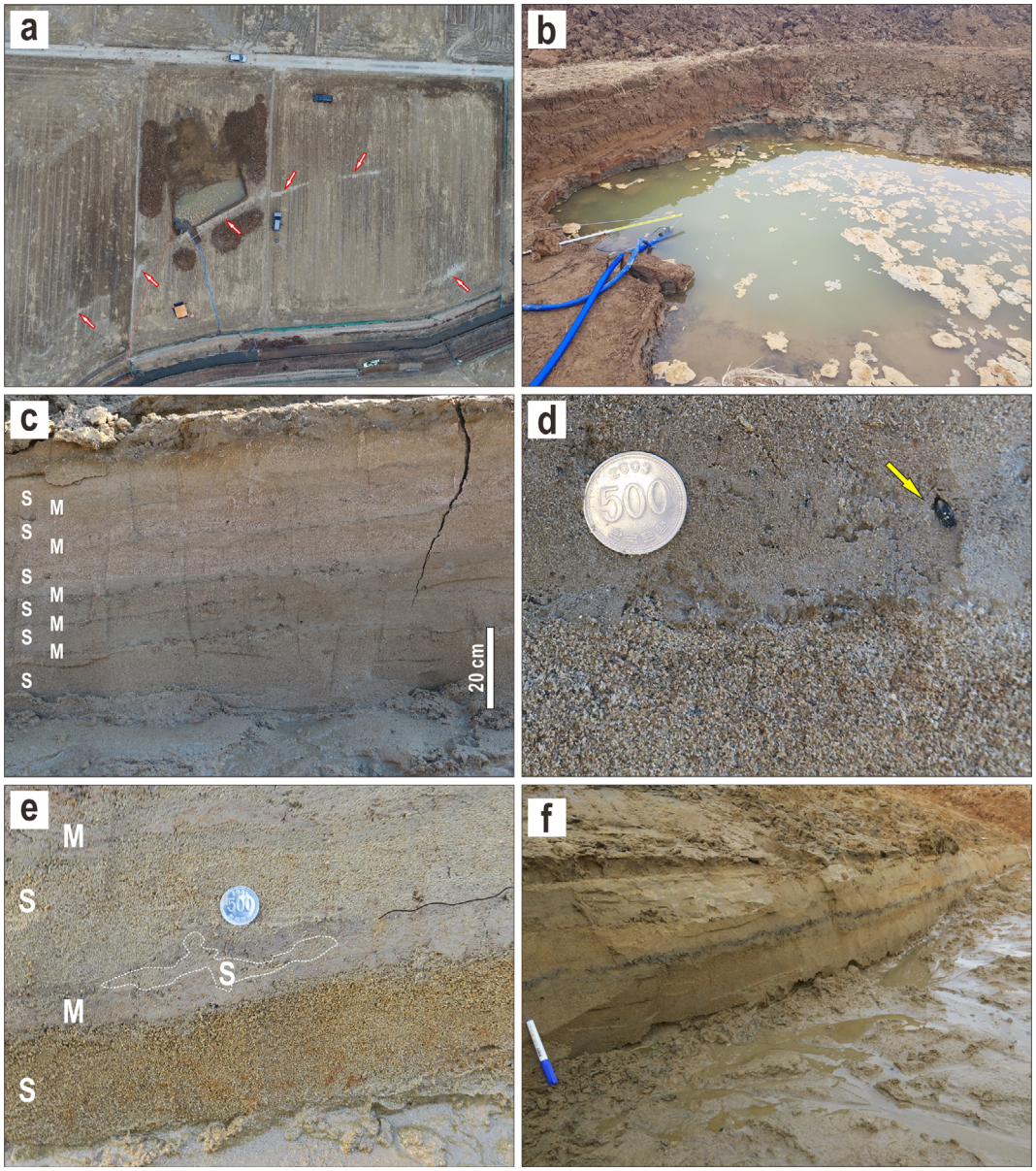

Fig. 6. Photographs of the trench site (a and b) and the Quaternary sediments (c–f). (a) A drone image of the trench site. The trench site is located in the area where linear sand blows occur. (b) High discharge of the ground water. The rapid release of the groundwater caused ground instabilities and hampered deep excavation. (c) Unit B composed of interbedded sand and mud. (d) A charcoal fragment in the sand bed in Unit B. (e) Close-up view of Unit B. The sand beds decrease in grain size upwards and are overlain by thin mud layers. (f) Lateral continuity of the interface between sand and mud layers in Unit B.

medium sand). The lower boundary of the sand layer is sharp and rounded pebbles are found near the lower boundary. Carbonized wood fragments are common in the sand layers (Fig. 6d), with ^{14}C radiocarbon ages estimated at 730 to 130 yrs BP. Each sand bed is massive and structureless overall, but in the uppermost part of each bed, grain size decreases upward, capped by a few cm thick grey mud layers (Fig. 6e). The boundary between mud and sand layers is either sharp or gradual, but generally undulatory due to the development of a series of load and water-escaped structures; these boundaries can be traced along the entire trench wall (< 15 m) (Fig. 6f).

Normal grading and lateral continuity as well as occurrence of two meandering streams near the trench site (Fig. 1) suggest that the sand layers in Unit B were deposited by decelerating sheetfloods across a floodplain (Miall, 1996). The overlying mud layers in Unit B are interpreted to have been deposited by suspension settling of silt and clay particles from stagnant waterbody on the floodplain (Carling, 2013). Although the overall massive structure of Unit A makes it difficult to elucidate the depositional processes, its mud-prone nature and scattered pebbles as well as the lack of sandy layer may indicate artificial molding of the mud on Unit B for agricultural purposes.

https://doi.org/10.1007/s12303-018-0051-y

3.2. Soft Sediment Deformation Structures (SSDSs)

Water-escaped and load structures are well-developed within the trench site. Such structures are generally formed by subsurface deformation during liquefaction and are collectively referred to as soft sediment deformation structures (SSDSs) (Allen, 1982; Owen, 1987, 1996). SSDSs also include sand blows that are produced by sediments vented from the subsurface to the surface through water-escaped structures (Owen, 2003). These structures are formed as a result of upward movement of pressurized pore water (fluidization) during and immediately after liquefaction (Owen et al., 2011). Upward-moving water typically carries sediments, so water-escaped structures can be recognized by vertical or subvertical alignments of exotic sediments, such as sand or mud dikes.

In our trench site, sand dikes are commonly observed in Unit A (Fig. 7a). These consist of very fine to medium sand and generally show sinuous patterns ranging from a few to 10 cm wide (Fig. 7b). These are often rootless in cross section, but at the boundary between Units A and B, some were clearly sourced from the sand layers in Unit B (Fig. 7c). This indicates that the sand layers in Unit B were likely the source of the sand blows

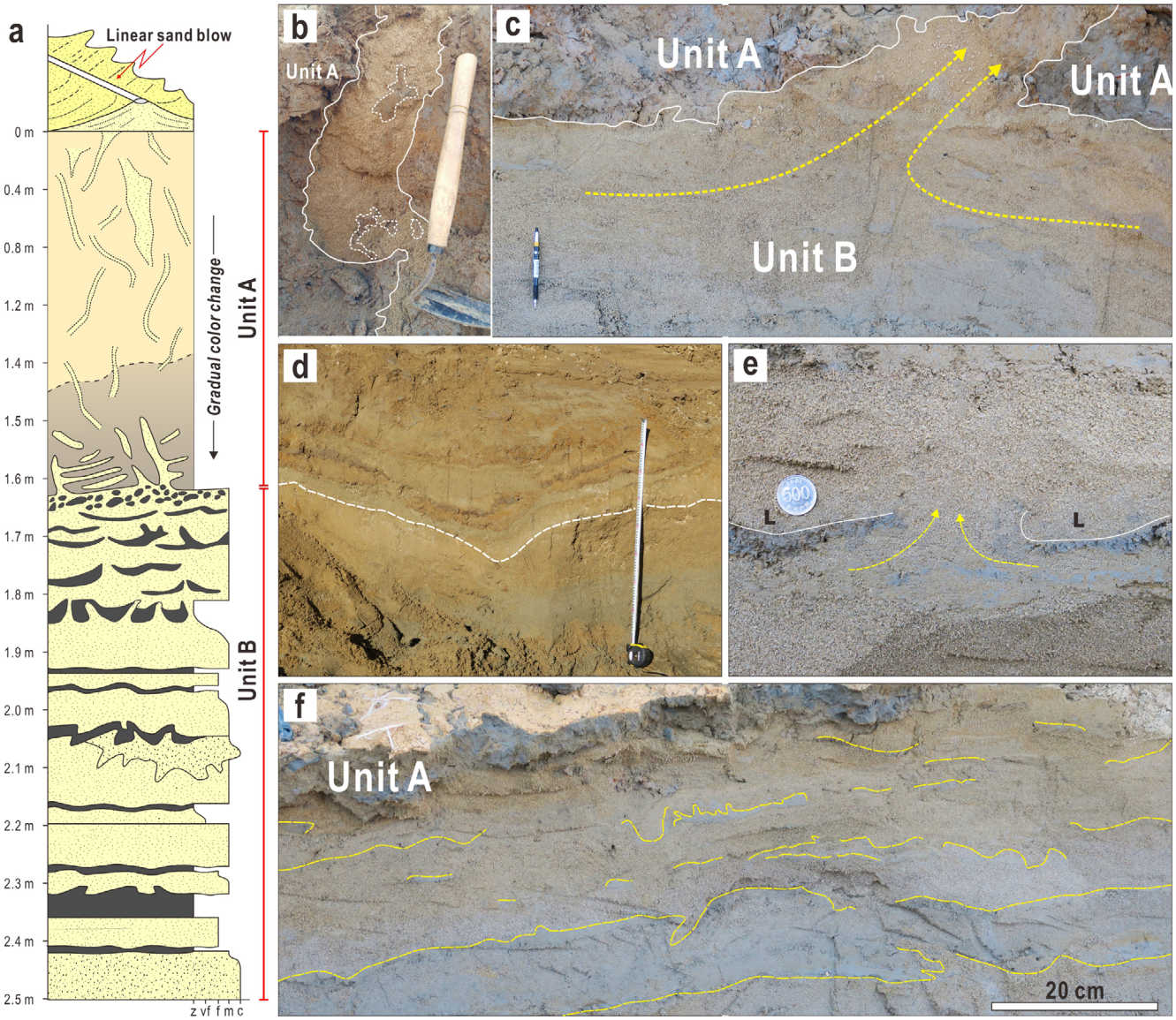

Fig. 7. Columnar log of the trench site and photographs of the soft sediment deformation structures (SSDSs) at the trench site. (a) Stratigraphic log of the sediments. The sediments can be divided into Unit A and B on the basis of the grain size and stacking patterns. Sand and mud interfaces in Unit B are highly deformed by the developments of a series of soft sediment deformation structures. (b) Rootless sand dike in Unit A. (b) A sand dike at the interface between Unit A and B. (c) A large load structure. Distorted lamina and beds parallel to border of the load structures are noteworthy. (d) Load and water-escaped structures at the boundary between sand and mud layers. The water-escaped structures occur commonly between the load structures (L: load structures) (e) Broken and highly deformed interfaces (dashed lines) between sand and mud layers slightly below the Unit A.

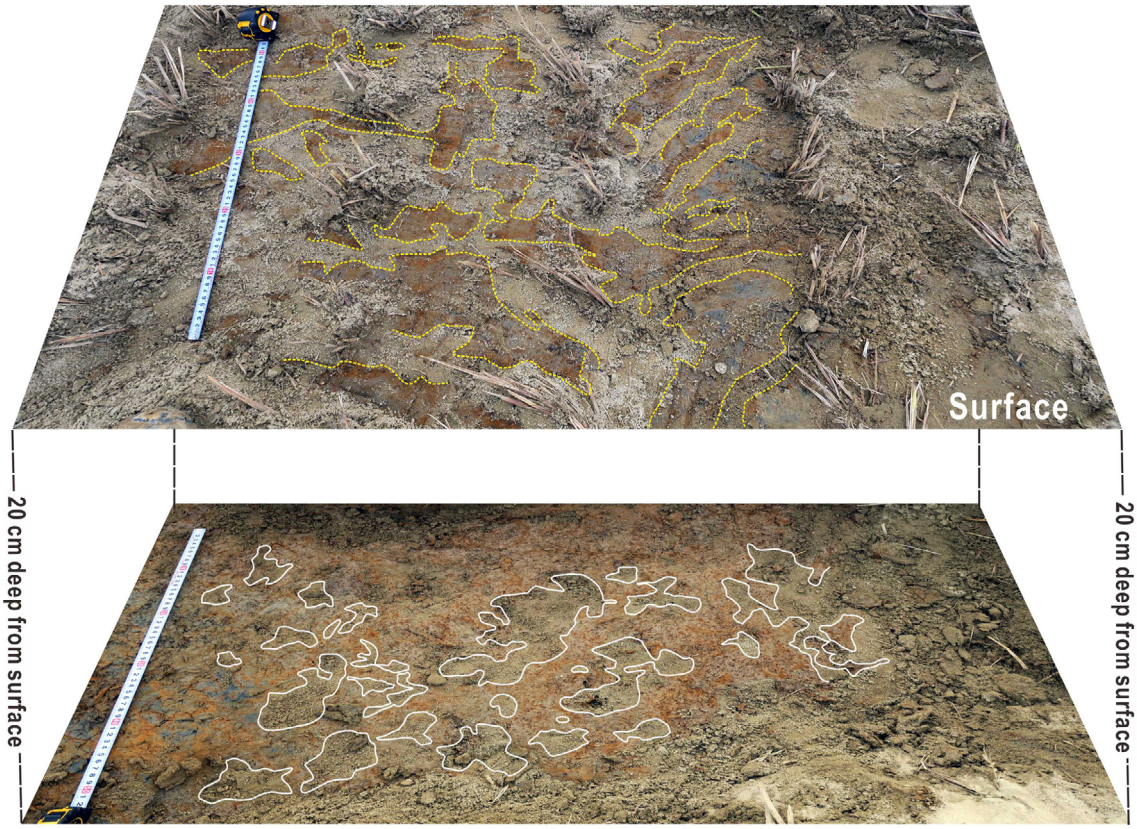

Fig. 8. Plan view of the sand dikes in Unit A. Whereas the sand dikes 20 cm below the surface show highly irregular geometry and are isolated each other, those on the surface intersect each other, exhibiting reticular patterns.

developed on the surface. In plain view, these sand dikes are spherical or semi-spherical in shape with irregular boundaries beneath the surface and are isolated from each other. However, on the surface, they increase in width and are interconnected in a more reticular pattern (Fig. 8).

The load structures are developed in a reverse density gradient system (e.g., Rayleigh-Taylor instability) (Owen, 2003). During liquefaction, the sediments lose their strength and behave as a semi-liquid state. Thus, downward movement of the overlying heavy sediments (typically sand) into the underlying light sediments (typically silt and clay) results in the formation of the sinuous boundary between the sediments (load structures). These structures are common at the interface between the overlying sand and underlying mud layers in Unit B (Fig. 6f) and are composed of very fine to coarse sand with gently concave-up, semi-spherical to spherical shapes with sharp or irregular margins ranging in width from a few cm to 40 cm. In larger cases, bedding planes are also contorted parallel to the borders of large load structures (Fig. 7d). Water-escaped structures are occasionally present between the load structures (Fig. 7e). In addition, in the lower part of Unit B, the load structures only exhibit sinuous boundaries, whereas in the uppermost part of Unit B, the bedding and lamina have typically been destroyed by a series of load and water-escaped structures (just below the boundary between Units A and B) (Figs. 7a and f).

4. DISCUSSION

4.1. Evaluation of Underground Conditions for Liquefaction

Seismogenic liquefaction occurs in unconsolidated or poorly consolidated sediments (such as the Quaternary sediments in this study) and is triggered by ground motions during an earthquake (Obermeier, 2009). Earthquake magnitude and duration are the most important factors for liquefaction, which is closely related to the areal extent of sand blows (Galli, 2000). However, even during strong earthquakes, sand blows occurs only under suitable underground conditions. The favorable ground conditions for liquefaction are summarized in Table 1 (Obermeier, 2009; Owen and Moretti, 2011).

At the trench site, water-escaped structures vertically connected with a linear sand blow on the surface indicate that sand beds in Unit B were liquefied during the earthquake. These sand beds are composed of very fine to coarse sand (mainly medium sand), which is close to the optimum grain size for liquefaction

https://doi.org/10.1007/s12303-018-0051-y

Table 1. A comparison of sediment characteristics in the trench site with optimum sediment conditions for liquefaction (after Obermeier, 2009; Owen and Moretti, 2011)

Factors	Optimum conditions	Trench site
Grain size	Coarse silt to medium sand	Fine to coarse sand (mostly medium sand)
Saturation	Saturation	Saturation (GW discharge 1.6 m below surface)
Packing degree	Loose	Soft (scrapped by finger)
Impermeable cap	Present	Present (mud layers in Unit B and overlying Unit A)
Overburden pressure	Low (< 10 m)	Low (1.6 m thick (Unit A))

(Obermeier, 2009). The sand beds in Unit B would be fully water-saturated at the time, because groundwater was released from the topmost sand bed (1.5–1.6 m below the surface).

The sand in these beds is also quite soft, suggesting that during liquefaction, the weight of individual sand grains could have been supported freely by increased pore water pressure. In addition, the liquefied sand beds were confined by underlying and overlying mud layers that prevented drainage of the pressurized water leading to a drastic increase in pore water pressure. Lastly, Unit B is overlain by the thin but impermeable Unit A (hence, low overburden pressure). When the increased pore water pressure exceeded the sediment strength of Unit A, the pore water and its sediments readily moved vertically through Unit A and was eventually vented onto the surface. As a result, water-escape structures readily developed in Unit A together with resultant sand blows on the surface (Rodríguez-Pascua et al., 2015). Several lines of evidence suggest that ground conditions around the epicenter were favorable for liquefaction (Table 1), resulting in the dense and widespread occurrence of sand blows despite the moderate magnitude of the 2017 Pohang Earthquake.

4.2. Paleoseismological Implications of the Liquefaction-induced Structures

Surface ruptures and resultant Quaternary faults play a key role in understanding the recurrence intervals of strong earthquake (> M_w 6.0) and assessing the long-term seismic hazards in the given region. After the two recent significant earthquakes in South Korea (the 2016 Gyeongju and 2017 Pohang earthquakes), heightened concerns regarding seismic hazards have highlighted the need for reliable paleoseismological information. The Korean government has initiated further research on active faults which have potential to be activated in the near future. This project is largely based on mapping the Quaternary faults by tracing tectonically deformed geomorphic features (Burbank and Anderson, 2011). This is because the elements, such as length, slip per event, and slip-rate, can provide invaluable paleoseismological information on earthquake magnitude and potential intensity (Wells and Coppersmith, 1994) as well as recurrence intervals through trench surveys (McCalpin, 2009).

In South Korea, however, researchers are commonly faced with problems when using this approach. Due to the region's intraplate setting, its faults are considered to be relatively slow-moving and large surface ruptures are rare compared to more active tectonic regions. Even where surface ruptures occur, summer rainfall events can obscure the geomorphic markers, complicating the detection and mapping of these faults. In addition, Quaternary landforms in and around metropolitan cities, particularly in SE Korea, have also been destroyed by high-density development and land use. Therefore, it is difficult to extract reliable paleoseismological information. Moreover, as it is commonly believed that earthquakes exceeding M_w 6.0 lead to surface ruptures (Bonilla, 1988), it is more difficult to identify the physical evidence for moderate but still damage-inducing earthquakes (5.0 < M_w < 6.0); for example the 2016 Gyeongju and 2017 Pohang earthquakes. All of these factors make difficulties for examining the history of paleoearthquakes in a given fault system.

Liquefaction is a common phenomenon during moderate to strong earthquakes (M_w > 5.0) and the areal extent of related surficial structures is largely associated with magnitude (Galli, 2000; Tuttle et al., 2002; Castilla and Audemard, 2007). Liquefaction-induced structures can therefore provide paleoseismological information such as prehistoric recurrence intervals and minimum magnitude. For instance, Tuttle et al. (2002) documented the earthquake calendars of the New Madrid Seismic Zone in the U.S. based on distributions of sand blows and their radiocarbon ages. Galli (2000) investigated the relationship between earthquake magnitude and the areal extent of liquefaction-induced structures using historical seismicity and reported sand blow locations. These studies suggest that moderate (< M_w 6.0) earthquakes can produce liquefaction-induced structures less than 20 km from the epicenter. Thus, the sand blows could be unique records of paleoearthquakes, because surface ruptures are commonly involved by earthquakes larger than magnitude 6.0 (Bonilla, 1988).

The 2017 Pohang Earthquake produced a number of sand blows. Despite its relatively moderate magnitude (M_w 5.4), the extent of sand blows (up to 15 km from the epicenter) demonstrated the wide-ranging influence of liquefaction, in good agreement with the work of Galli (2000). This liquefaction also involved

subsurface deformation and resultant SSDS formation in the Quaternary sediments. Both their wide occurrence and subsurface development suggest that SSDSs may act as one of main tools in investigating paleoearthquakes. This kind of record in subsurface is also able to endure for surface erosional processes, having a higher preservational potential than geomorphic markers. This strongly indicates that SSDSs have the potential to serve as prehistoric earthquake evidence in South Korean, particularly in moderate earthquakes that make SSDS but not involve vivid surface rupture (Fig. 9).

Despite these advantages, paleoseismological studies based on SSDSs will also have limitations. First, because liquefaction is triggered by ground motion during earthquakes, it is impossible to determine the kinematics and precise locations of casual faults. Second, although previous research suggests that types of SSDSs are related to earthquake magnitude (Rodríguez-Pascua et al., 2000), it is difficult to determine the magnitude of the causal earthquakes because the deformation complexity and resulting types of SSDSs are also affected by the duration of liquefaction along with the water content and thickness of the liquefied beds (Owen and Moretti, 2011).

However, the relatively low thresholds for development of liquefaction-induced structures are still helpful for detecting evidence of damage-inducing earthquakes (> M_w 5.0) that did not produce surface ruptures, such as the 2016 Gyeongju and 2017 Pohang Earthquakes (Fig. 9). Furthermore, our trench site showed that episodic flooding events and consequent sediment profiles in floodplains can produce suitable conditions for liquefaction from even a moderate (> M_w 5.0) earthquake (Table 1). In South Korea, a number of people are now living in these environments. Thus, it is particularly necessary to study SSDSs in these areas to determine the recurrence intervals of prehistoric earthquakes with damage-inducing magnitudes (> M_w 5.0). We conclude that combining SSDS and active fault researches can overcome their individual limitations; this is necessary to provide reliable paleoseismological information in South Korea. Also, for other intraplate and tropical regions, we argue that collaborative researches (both Quaternary faults and SSDSs) could be very helpful to evaluate the prehistoric earthquakes and to assess seismic hazard.

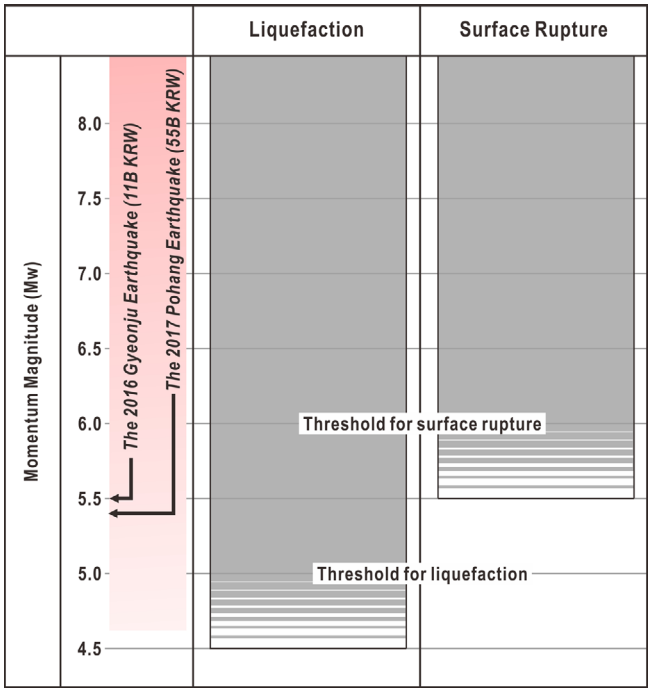

Fig. 9. A comparison between threshold for the development of liquefaction and surface rupture with the recent damage-inducing earthquakes in the Korean Peninsula. Estimated damages are in parentheses.

5. CONCLUSIONS

(1) We identified approximately 600 sand blows that formed immediately after the 2017 Pohang Earthquake (M_w 5.4) in South Korea. Most are distributed within 3 km of the epicenter, with the farthest 15 km away.

(2) These sand blows are classified into subcircular, linear, and linear along an artifact on the basis of their morphology. The linear type which is the majority of the sand blows preferentially oriented NNE-SSW.

(3) We performed a trench survey at a selected sand blow site to better understand the ground's susceptibility to liquefaction. Sediment profile conditions below the sand blows (including grain size, groundwater level, overburden pressure, and impermeable cap) are consistent with conditions favoring seismic-induced liquefaction.

(4) A number of soft sediment deformation structures (SSDSs) such as load and water-escape structures are well-developed below the sand blow in our trench site. These suggest that liquefaction caused by the 2017 Pohang Earthquake resulted in both sediment extrusion to the surface and subsurface deformation.

(5) The genetic linkage between SSDSs (including sand blows) and earthquakes suggests that research on SSDSs in South Korea should be undertaken to identify evidence of prehistoric earthquakes. This research could reveal prehistoric earthquakes of a sufficient magnitude to produce damage but below the threshold required to produce visible surface ruptures (5.0 < M_w).

(6) The high preservational potential of subsurface SSDSs can therefore overcome the limitations of active fault research by providing an additional tool for the identification and analysis of earthquake history with respect to modern seismic hazards. Thus, combined studies of active faults and SSDSs are necessary to provide reliable and useful paleoseismological information in South Korea.

https://doi.org/10.1007/s12303-018-0051-y

ACKNOWLEDGMENTS

This work is supported by a project "Research on geologic hazard assessment of large fault system – focusing on central region of the Yangsan Fault" funded by Ministry of Science and ICT. We are grateful for constructive comments of two reviewers (Prof. M. Son and anonymous) and editorial handling of the Editor (Prof. J. Rhie).

REFERENCES

Allen, J.R.L., 1982, Sedimentary Structures: Their Character and Physical Basis (Vol. II). Elsevier, Amsterdam, 663 p.

Bonilla, M.G., 1988, Minimum earthquake magnitude associated with coseismic surface faulting. Bulletin of the Association of Engineering Geology, 25, 17–29.

Burbank, D.W. and Anderson, R.S., 2011, Tectonic Geomorphology (2nd edition). John Wiley and Sons, Chichester, 454 p.

Carling, P.A., 2013, Freshwater megaflood sedimentation: What can we learn about generic processes? Earth-Science Review, 125, 87–113.

Castilla, R.A. and Audemard, F.A., 2007, Sand blows as a potential tool for magnitude estimation of pre-instrumental earthquakes. Journal of Seismology, 11, 473–487.

Galli, P., 2000, New empirical relationships between magnitude and distance for liquefaction. Tectonophysics, 324, 169–187.

Hwang, I.G., Chough, S.K., Hong, S.W., and Choe, M.Y., 1995, Controls and evolution of fan delta systems in the Miocene Pohang basin, SE Korea. Sedimentary Geology, 98, 145–179.

KIGAM, 2018, Earthquakes in the Southeast Korean Peninsula: focusing on the 2016 Gyeongju and the 2017 Pohang Earthquakes. Korea Institute of Geoscience and Mineral Resources, Daejeon, 56 p.

Kim, Y.-S. and Jin, K.M., 2006, Estimated earthquake magnitude from the Yugye Fault displacement on a trench section in Pohang, SE Korea. Journal of the Geological Society of Korea, 42, 79–94. (in Korean with English abstract)

Kyung, J.B. and Chang, T.-W., 2001, The Latest Fault Movement on the Northern Yangsan Fault Zone around the Yugye-Ri Area, Southeast. Journal of the Geological Society of Korea, 37, 563–577. (in Korean with English abstract)

Maltman, A.J. and Bolton, A., 2003, How sediments become mobilized. In: Van Rensbergen, P., Hillis, R.R., Maltman, A.J., and Morley, C.K. (eds.), Subsurface Sediment Mobilization. Geological Society, London, Special Publications, 216, p. 9–20.

McCalpin, J.P., 2009, Paleoseismology (2nd edition). Academic Press, San Diego, 613 p.

Miall, A.D., 1996, The Geology of Fluvial Deposits. Springer, Berlin, 582 p.

Obermeier, S.F., 1996, Use of liquefaction-induced features for paleoseismic analysis – an overview of how seismic liquefaction features can be distinguished from other features and how their regional distribution and properties of source sediment can be used to infer the location and strength of Holocene paleo-earthquakes. Engineering Geology, 44, 1–76.

Obermeier, S.F., 2009, Using liquefaction-induced and other soft-sediment features for paleoseismic analysis. In: McCalpin, J.P. (ed.), Paleoseismology (2nd edition). Academic Press, London, p. 497–564.

Owen, G., 1987, Deformation processes in unconsolidated sands. In: Jones, M.E. and Preston, R.M.F. (eds.), Deformation of Sediments and Sedimentary Rocks. Geological Society, London, Special Publications, 29, p. 11–24.

Owen, G., 1996, Experimental soft-sediment deformation: structures formed by the liquefaction of unconsolidated sands and some ancient examples. Sedimentology, 43, 279–293.

Owen, G., 2003, Load structures: gravity-driven sediment mobilization in the shallow subsurface. In: Van Rensbergen, P., Hillis, R.R., Maltman, A.J., and Morley, C.K. (eds.), Subsurface Sediment Mobilization. Geological Society, London, Special Publications, 216, p. 21–34.

Owen, G. and Moretti, M., 2011, Identifying triggers for liquefaction-induced soft-sediment deformation in sands. Sedimentary Geology, 235, 141–147.

Owen, G., Moretti, M., and Alfaro, P., 2011, Recognising triggers for soft-sediment deformation: current understanding and future directions. Sedimentary Geology, 235, 133–140.

Rajendran, K., Rajendran, C.P., Thakker, M., and Tuttle, M.P., 2001, The 2001 Kachchh (Bhuj) earthquake: coseismic surface features and their significance. Current Science, 80, 1397–1405.

Rodríguez-Pascua, M.A., Calvo, J.P., De Vicente, G., and Gomez Gras, D., 2000, Soft sediment deformation structures interpreted as seismites in lacustrine sediments of the Prebetic Zone, SE Spain, and their potential use as indicators of earthquake magnitudes during the Late Miocene. Sedimentary Geology, 135, 117–135.

Rodríguez-Pascua, M.A., Silva, Pablo G.P.G., Perez-Lopez, R., Giner-Robles, J.L., Martín-Gonzalez, F., and Del Moral, B., 2015, Polygenetic sand volcanoes: on the features of liquefaction processes generated by a single event (2012 Emilia Romagna 5.9 Mw earthquake Italy). Quaternary International, 357, 329–335.

Sims, J.D., 1975, Determining earthquake recurrence intervals from deformational structures in young lacustrine sediments. Tectonophysics, 29, 141–152.

Sohn, Y.K. and Son, M., 2004, Synrift stratigraphic geometry in a transfer zone coarse-grained delta complex, Miocene Pohang Basin, SE Korea. Sedimentology, 51, 1387-1408.

Son, M., Song, C.W., Kim, M.-C., Cheon, Y., Cho, H., and Sohn, Y.K., 2015, Miocene tectonic evolution of the basins and fault systems, SE Kora: Dextral, simple shear during the East Sea (Sea of Japan) opening. Journal of the Geological Society, 172, 664–680.

Tuttle, M.P., Schweig, E.S., Sims, J.D., Lafferty, R.H., Wolf, L.W., and Haynes, M.L., 2002, The earthquake potential of the New Madrid seismic zone. Bulletin of the Seismological Society of America, 92, 2080–2089.

Wells, D.L. and Coppersmith, K.J., 1994, New empirical relationships among magnitude, rupture length, rupture width, rupture area, and surface displacement. Bulletin of Seismological Society of America, 84, 974–1002.